Tuijin Jishu/Journal of Propulsion Technology
ISSN: 1001-4055
Vol. 44 No. 5 (2023)

Peristaltic transport of Jeffrey Fluid in a Doubly Connected Region

[1]Priyanka N B, [2]Indira R, [3]Jagadeesha S

[1]Department of Mathematics, ATME College of Engineering, Mysuru and Visvesveraya Tehnological University, Belagavi-590018, India
[2] [3] Department of Mathematics, Nitte Meenakshi Institute of Technology, Bengaluru and Visvesveraya Tehnological University, Belagavi-590018 India

Abstract: A porous vertical annulus subjected to a peristaltic wave motion on the outer wall is considered. Heat transfer in Jeffrey fluid flowing in an annular region is considered. A wave frame of reference is assumed here. The governing equations are subjected to long wavelength approximation and low Reynold's flow. The velocity and pressure gradient are evaluated by applying regular perturbation. The friction at the wall and pressure rise are numerically evaluated and graphically depicted. As $\lambda \to 0$, the solution reduces to Newtonian fluid.

1. Introduction

Peristaltic action is a very effective mode of transport that occurs in the human body. The passage of urine, chime, food bolus etc. are due to peristaltic motion of the walls of the vessels. The mechanism has been effectively adopted for designing pumps for the transport of corrosive fluids. Many authors have analyzed experimentally and numerically the peristalsis in the reproductive system [1]-[6]. Newtonian fluid has been considered to study peristalsis by many authors [7] and [3]. Peristaltic transport of embryos was analyzed by Misra et. al [8], Li et. al [9].Many authors have considered the theoretical study of peristaltic transport. Eytan et. al [10], Mishra et. al [11] and Li et. al [9] have analyzed the effect of peristaltic flow on Newtonian fluids in different geometries like rectangular channels, cylindrical tubes, assuming uniformity, and non-symmetric geometries theoretically. Misra et. al [12], Shukla et. al [13] and Raju et. al [14] have analyzed Power-law fluid under peristaltic transport. They have considered a uniform channel with axi-symmetry subjected to a sine wave.

A uniform tube under peristaltic motion is analyzed by considering axisymmetric flow of Casson fluid by Mernone et. al [15]. Heat transfer effects on axisymmetric flow of Power-law fluid with chemical reaction is studied by Hayat et. al [16] and Eldabe et. al [17]. A concentric porous annulus with peristaltic transport under the influence of a magnetic field is considered by Shaaban et. al [18].

Selvi et. al [19] and Ahmed et. al [20] have studied the effect of peristalsis on Jeffrey fluid flow analytically. The flow of couple-stress fluid in an asymmetric channel under peristaltic motion was considered by Sreegowrav et. al [21]. Rashmi et. al [22] have studied peristaltic transport of couple-stress fluid analytically in an eccentric annulus. Effects of heat transfer in a peristaltic transport of Prandtl fluid flowing in av ertical annulus is investigated by Indira et. al [23]. A porous annulus vertically placed is considered and heat transfer in peristaltic transport is studied using perturbation by Vajravelu et. al [24].

In the present study, an attempt is made to understand the effect of heat transfer on peristaltic transport of Jeffrey fluid in a vertical annulus. The method of regular perturbation is employed along with low Reynold's number and a long wavelength approximation.

2. Mathematical Formulation

A vertical annulus with the X axis as its axis is placed as shown in the figure. The cylindrical tubes are placed concentrically. A sinusoidal wave is applied to the outer wall with long wavelength approximation. The temperatures on the walls are T_0 and T_1 respectively. The walls deform according to the function:

$$H(x,t) = a_0 + b\sin\left(\frac{2\pi}{\lambda}\right)(X - ct)$$

where a_0 - radius of outer tube in absence of sine wave, b - amplitude, $\lambda -$ wavelength and $c -$ wave velocity.

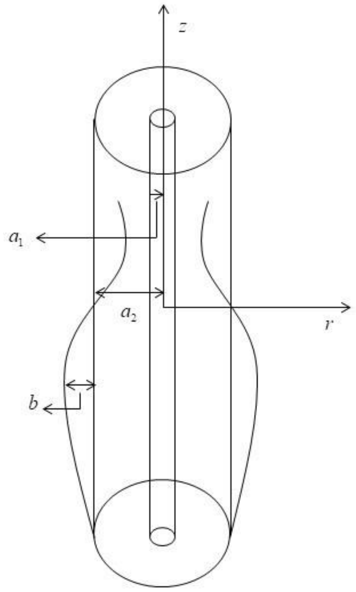

Figure 1: Physical configuration

The governing equations for the above configuration assuming Jeffrey fluid flowing in the annular region can be stated as,

$$\rho \frac{d\vec{q}}{dt} = \nabla \cdot \vec{r} + \rho \vec{F} - \frac{\mu}{k}\vec{q}, \tag{1}$$

$$\nabla \cdot \vec{q} = 0, \tag{2}$$

and $$\vec{\tau} = -PI + S, \quad S = \frac{\mu}{(1+\lambda_1)}\left(\dot{\gamma} + \lambda_2 \ddot{\gamma}\right), \tag{3}$$

$$\rho c_f \frac{dT}{dt} = k\nabla^2 T + \mu\varphi + \frac{\mu}{k_0}\vec{q}^{\,2}, \tag{4}$$

where $\vec{q}-$ velocity, $\rho-$ density, $\rho c_f -$ heat capacity, $\phi -$ viscous dissipation,

$\tau -$ Cauchy's stress tensor, $\vec{F} -$ body force, $\lambda_1 - \dfrac{\text{relaxation time}}{\text{retardation time}}$, $\lambda_2 -$ retardation time and $\gamma -$ shear rate.

The equations above are subjected to,

$$w = 0 \text{ at } R = a_1 \text{ and } R = H(x,t), \tag{5}$$

$$T = T_1 \text{ at } R = a_1 \text{ and } T = T_0 \text{ at } R = H. \tag{6}$$

A moving frame of reference is introduced using velocity c of the wave and assuming, $w = W - c,\ r = R,\ z = Z - ct,$ and implementing non-dimensionalizing the above equations using the parameters, and neglecting the asterisks $(*)$,

$$z^* = \frac{z}{\lambda},\ r^* = \frac{r}{a_0},\ p^* = \frac{a^2 p}{\lambda\mu c},\ u^* = \frac{\lambda\mu}{ac},\ t^* = \frac{ct}{\lambda},\ w^* = \frac{w}{c},\ \theta^* = \frac{T - T_0}{T_1 - T_0},\ \varepsilon = \frac{b}{a_0},\ S^* = \frac{aS}{\mu c},$$

$$r_1^* = \frac{r_1}{a},\ \mathrm{Re} = \frac{\rho ca}{\mu},\ \delta = \frac{\lambda}{a},\ G_m = \frac{\rho g \alpha a^2 (T - T_0)}{\mu c},\ E_m = \frac{c^2}{k(T_1 - T_0)},$$

We get,

$$-\frac{\partial p}{\partial r} = 0, \tag{7}$$

$$0 = -\frac{\partial p}{\partial z} + \frac{1}{r}\frac{\partial}{\partial r}(rS_{rz}) - \sigma^2 (w+1) + G_m \theta, \tag{8}$$

$$0 = \frac{\partial w}{\partial z} + \frac{1}{r}\frac{\partial}{\partial r}(u_r), \tag{9}$$

$$S_{rz} = \frac{\partial w}{\partial r}, \tag{10}$$

$$0 = \frac{1}{r}\frac{\partial}{\partial r}\left(r\frac{\partial r}{\partial \theta}\right) + E_m\left(\frac{\partial w}{\partial r}\right)^2 + \sigma^2 E_m (w+1)^2,$$

and $\eta(x) = 1 + \varepsilon \sin 2\pi x$. (11)

The boundary conditions take the form:

$w = -1$ on $r = r_1$ and on $r = \eta(x)$, (12)

$\theta = 1$ on $r = r_1$ and $\theta = 0$ on $r = \eta(x)$. (13)

The governing equations are coupled and non-linear. A regular perturbation technique with porosity σ^2 and convection parameter G_r is assumed as,

$$g = (g_{00} + G_m g_{01} + \ldots) + \sigma^2 (g_{10} + G_m g_{11} + \ldots), \tag{14}$$

where g is the variable representing velocity, pressure and temperature.

Applying perturbation scheme, the governing equations reduces to the following,

Equations of order zero:

$$0 = -\frac{\partial p_{00}}{\partial x} + \left[\frac{1}{1+\lambda_1}\right]\frac{1}{r}\frac{\partial}{\partial r}\left(r\frac{\partial w_{00}}{\partial r}\right), \tag{15}$$

$$0 = \frac{1}{r}\frac{\partial}{\partial r}\left(r\frac{\partial \theta_{00}}{\partial r}\right) + E_m\left(\frac{\partial w_{00}}{\partial r}\right)^2, \tag{16}$$

subject to,

$w_{00} = -1$ at $r = r_1$, $r = \eta(x)$,

$\theta_{00} = 1$ at $r = r_1$,

$\theta_{00} = 0$ at $r = \eta(x)$. (17)

Equations of order one:

$$0 = -\frac{\partial p_{01}}{\partial x} + \frac{1}{r}\frac{\partial}{\partial r}\left(r\frac{\partial w_{01}}{\partial r}\right) + \theta_{00}, \tag{18}$$

$$0 = \frac{1}{r}\frac{\partial}{\partial r}\left(r\frac{\partial \theta_{01}}{\partial r}\right) + 2E_m\frac{\partial w_{00}}{\partial r}\frac{\partial w_{01}}{\partial r}, \tag{19}$$

subject to,

$$w_{01} = -1 \text{ at } r = r_1 \text{ , } r = \eta(x),$$
$$\theta_{01} = 0 \text{ at } r = r_1 \text{ ,}$$
$$\theta_{01} = 0 \text{ at } r = \eta(x). \tag{20}$$

and

$$0 = -\frac{\partial p_{10}}{\partial x} + \frac{1}{r}\frac{\partial}{\partial r}\left(r\frac{\partial w_{10}}{\partial r}\right) - (w_{00}+1), \tag{21}$$

$$0 = \frac{1}{r}\frac{\partial}{\partial r}\left(r\frac{\partial \theta_{10}}{\partial r}\right) + 2E_m\frac{\partial w_{00}}{\partial r}\frac{\partial w_{10}}{\partial r} + E_m(w_{00}+1)^2, \tag{22}$$

subjected to,

$$w_{10} = 0 \text{ at } r = a_1 \text{ , } r = \eta(x),$$
$$\theta_{10} = 0 \text{ at } r = a_1,$$
$$\theta_{10} = 0 \text{ at } r = \eta(x). \tag{23}$$

The solution of the above equations is given by,

$$w_{00} = -\left(\frac{1+\lambda_1}{4}\right)\frac{\partial p}{\partial x}\left[\eta^2(x) - r^2 + a_1\log\left(\frac{r}{\eta}\right)\right] - 1, \tag{24}$$

$$w_{01} = -E_m a_2^2(1+\lambda_1)\left[f(r,x) - f(\eta,x) - a_6\log\left(\frac{r}{\eta}\right)\right], \tag{25}$$

$$w_{10} = -(1+\lambda_1)a_2\left[f_3(r,x) - f_3(\eta,x) - a_7\log\left(\frac{r}{\eta}\right)\right], \tag{26}$$

where f, f_3 and constants are listed in the appendix.

The axial velocity is given by,

$$w = w_{00} + G_m w_{01} + \sigma^2 w_{10}. \tag{27}$$

The heat transfer is given by,

$$\theta_{00} = -E_m a_2^2\left[\frac{\eta^2 - r^2}{4} + a_1^2 + \log\left(\frac{r}{\eta}\right)\log(r\eta) - a_1(r^2-\eta^2)\right] + E_m a_2^2 a_3\frac{\log\left(\frac{r}{\eta}\right)}{\log\left(\frac{r_1}{\eta}\right)} + \frac{r-\eta(x)}{r_1-\eta(x)}, \tag{28}$$

$$\theta_{01} = 2E_m\left[f_1(\eta,x) - f_1(r,x) + \frac{f_1(r_1,x) - f_1(\eta,x)}{\log\left(\frac{r_1}{\eta}\right)}\log\left(\frac{r}{\eta}\right)\right]$$
$$+\left[f_2(r,x) - f_2(\eta,x) - \frac{f_2(r_1,x) - f_2(\eta,x)}{\log\left(\frac{r_1}{\eta}\right)}\log\left(\frac{r}{\eta}\right)\right], \tag{29}$$

$$\theta_{10} = E_m\left[f_4(r,x) - f_4(\eta,x) + \frac{f_4(r_1,x) - f_4(\eta,x)}{\log\left(\frac{r_1}{\eta}\right)}\log\left(\frac{r}{\eta}\right)\right], \tag{30}$$

$$\theta = \theta_{00} + G_m\theta_{01} + \sigma^2\theta_{10}. \tag{31}$$

The rate of flow in non –dimensional form can be written as,

$$Q = \int_0^{\eta} 2rwdr \quad \text{and} \quad Q = Q_{00} + G_m Q_{01} + ... + \sigma^2\left(Q_{10} + ...\right). \tag{32}$$

Using the equations from (24) to (27) in the equation (32) and rearranging we get pressure gradient in the form,

$$\frac{\partial p_{00}}{\partial x} = -\frac{\left(\frac{\eta^2 - r_1^2}{2}\right) + Q_{00}}{\left(1 + \frac{\lambda_1}{4}\right)\left(\frac{\eta^2 - r_1^2}{4}\right)\left(\eta^2 + r_1^2 + a_1^2\right)}, \tag{33}$$

$$\frac{\partial p_{01}}{\partial x} = \frac{E_m a_2^2(1+\lambda_1)b_1 - \left(\frac{\eta^2 - r_1^2}{2}\right) f(\eta,x) + a_6\left[\left(\frac{\eta^2 - r_1^2}{4}\right) + \frac{r_1^2}{2}\log\left(\frac{r_1}{\eta}\right)\right] - Q_0}{\left(\frac{1+\lambda_1}{4}\right)\left(\frac{\eta^2 - r_1^2}{4}\right)\left(\eta^2 + r_1^2 + a_1^2\right)}, \tag{34}$$

$$\frac{\partial p_{10}}{\partial x} = \frac{\frac{(1+\lambda_1)^2}{4}\left[\left(\frac{\eta^2 - r_1^2}{2}\right) f_3(\eta,x) - b_2 + a_1\frac{r_1^4}{4}\log\left(\frac{r_1}{\eta}\right) - \frac{a_1}{4}\left(\eta^2 - r_1^2\right)\right] - Q_0}{\left(\frac{1+\lambda_1}{4}\right)\left(\frac{\eta^2 - r_1^2}{4}\right)\left(\eta^2 + r_1^2 + a_1^2\right)}, \tag{35}$$

$$\frac{\partial p}{\partial x} = \frac{\partial p_{00}}{\partial x} + G_m\frac{\partial p_{01}}{\partial x} + \sigma^2\frac{\partial p_{10}}{\partial x}. \tag{36}$$

Between the walls, the pressure rise can be evaluated using,

$$\Delta p = \int_0^1 \frac{dp}{dz}dz. \tag{37}$$

3. Results and Discussion

A Jeffrey fluid flowing in a porous annulus formed by concentric cylinders with outer wall subjected to wave motion is considered. Inner and outer tubes are subjected to a temperature gradient. The flow is peristaltic, and a long wavelength approximation is applied. A perturbation solution for velocity, temperature, pressure is obtained numerically and graphically presented. The parameters arising out of the study are given values in the following literature.

Axial velocity profile as a function of radius is presented in figures 2 - 7 for various parameters available in the literature. Variation of axial velocity by increasing average flow rate is shown in figure 2, and since rate of flow is directly proportional to w, velocity increases with increasing Q and effect is significant. Figure 3 showcases the effect of the amplitude of peristaltic waves propagating on the outer wall. Axial velocity increases with increasing wave amplitude, but the effect is not very significant. The effect of temperature can be studied by analyzing the behavior of the Grashoff number G_m on velocity. As G_m increases, the velocity increases. As temperature increases, the resistance to flow decreases due to the reduction in viscosity; hence, there is a higher velocity. This can be seen in figure 4. The effect of permeability is analyzed in figure 5, and the effect is not very significant near the walls. As permeability increases, flow resistance decreases and velocity increases. The effect is stronger in the middle of the annular region. Figure 6 shows the effect of Eckert number on velocity. Eckert number gives the amount of heat dissipation. The effect of an increase in Eckert number is significant and results in increase of velocity. The velocity curve also shows tilting towards the inner wall. The increase in E_m is due to the increase in advective transport of heat, which results in a reduction of viscosity and an increase in velocity. Figure 7 depicts the effect of λ_1 on velocity. λ_1 - Jeffrey parameter is the ratio of relaxation to retardation time. As $\lambda_1 \to 0$, fluid tends to become Newtonian. As λ_1 increases, the velocity increases.

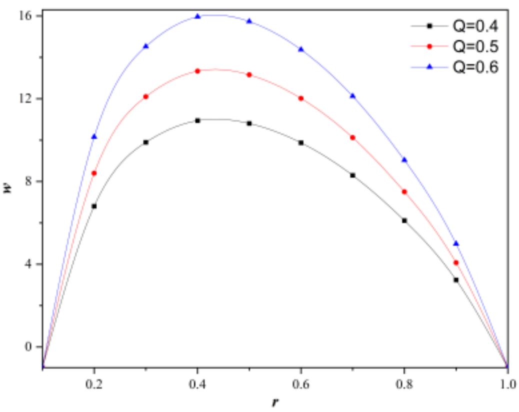

Figure 2: Axial velocity profile

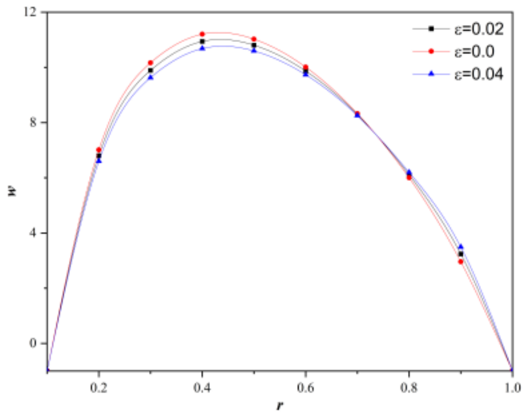

Figure 3: Axial velocity profile

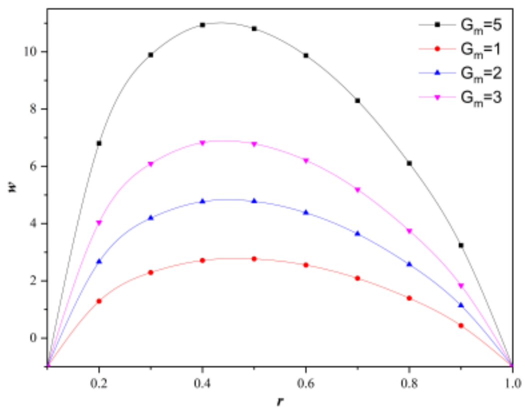

Figure 4: Axial velocity profile

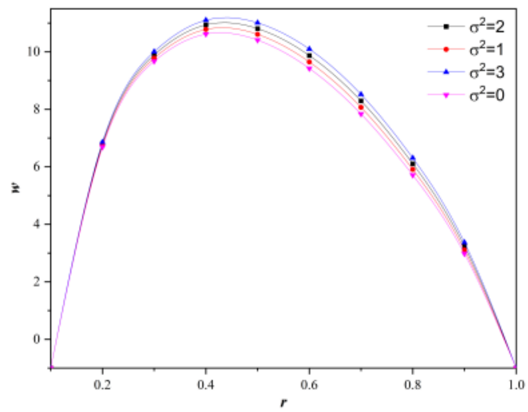

Figure 5: Axial velocity profile

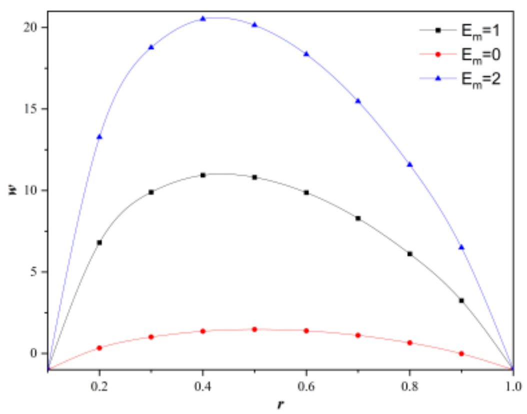

Figure 6: Axial velocity profile

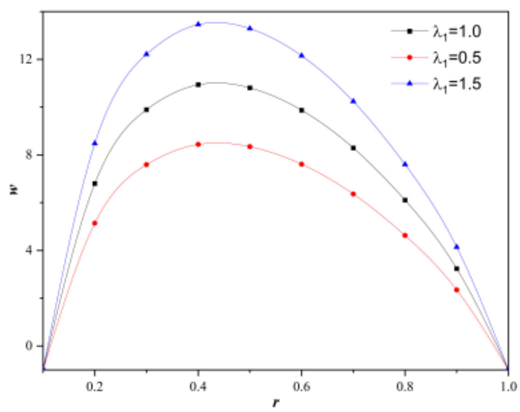

Figure 7: Axial velocity profile

Figure 8 presents axial velocity in axial direction for different Jeffrey parameter. As λ_1 increases magnitude of velocity increases.

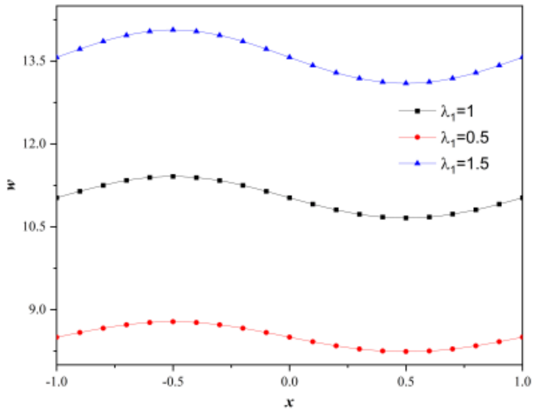

Figure 8: Axial velocity in axial direction

Figures 9 - 12 showcase the temperature in the radial direction for different parameters which reflects most of the same pattern as in the case of axial velocity. Temperature increases with increasing flow rate, Grashoff number, Jeffrey parameter, and Eckert number. As velocity increases, the advective transport of heat increases.

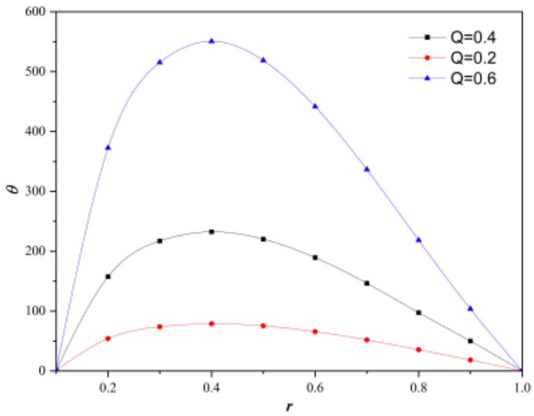

Figure 9: Radial temperature profile

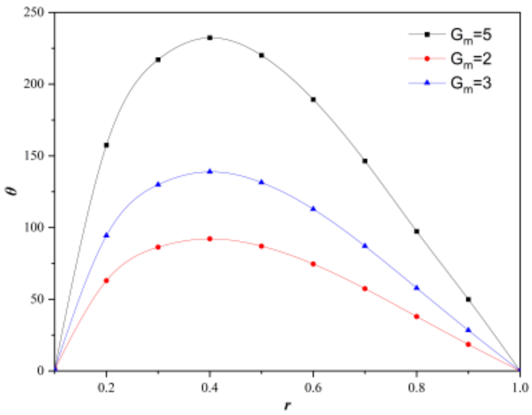

Figure 10: Radial temperature profile

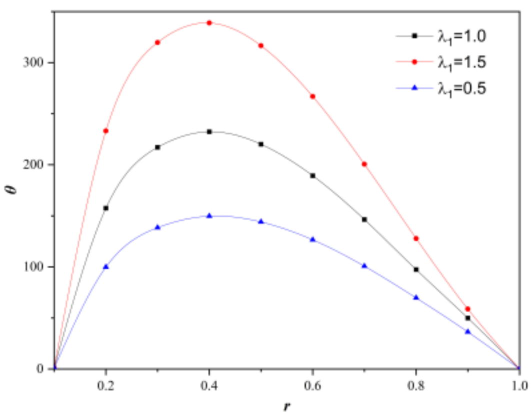

Figure 11: Radial temperature profile

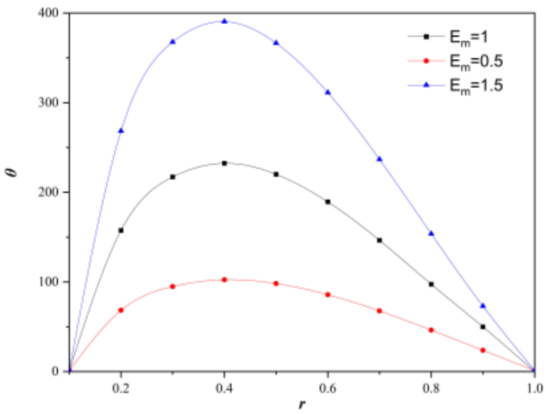

Figure 12: Radial temperature profile

Figures 13 - 17 depict the variation of the axial pressure gradient and as sine wave is propagating on outer wall, the pressure also shows same pattern. Pressure gradient increases with increasing rate of flow, Grashoff number, and Eckert number but decreases with increasing inner tube radius. As the inner tube radius increases, the area available for flow decreases, and pressure as well as velocity increases. As the permeability parameter increases, the resistance to flow decreases, and the pressure gradient increases.

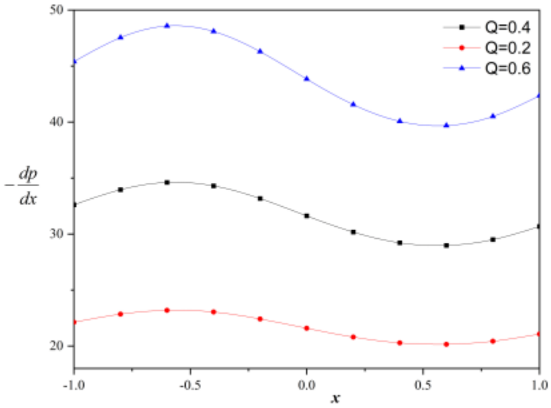

Figure 13: Axial pressure gradient

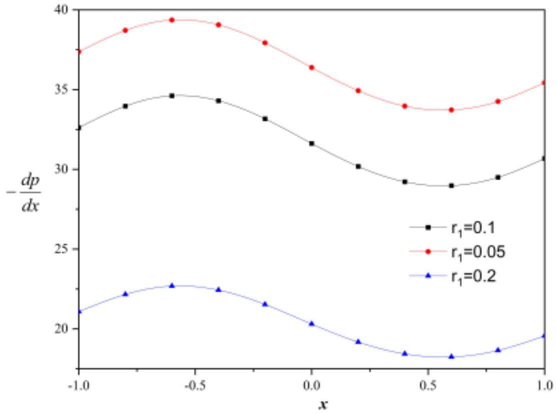

Figure 14: Axial pressure gradient

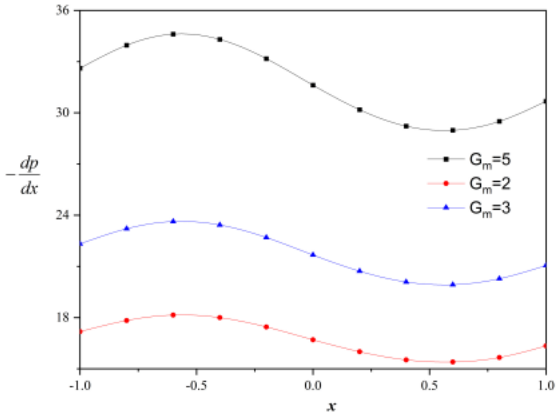

Figure 15: Axial pressure gradient

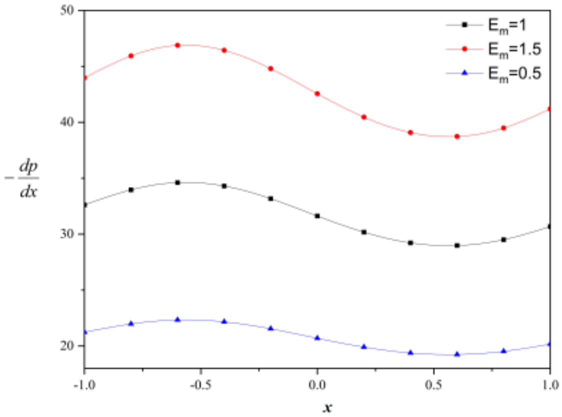

Figure 16: Axial pressure gradient

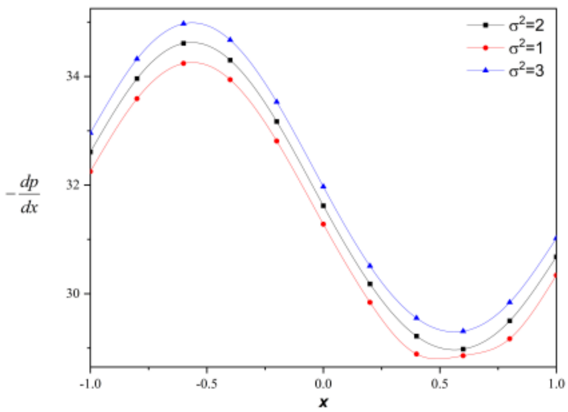

Figure 17: Axial pressure gradient

The rise of pressure between the walls against the flow rate is shown in figures 18 and 19. As inner tube radius increases, difference in pressure is more, and the pressure is negative between Q equal to 0.0 to 2.0. It shows that pressure decreases as the amplitude ratio increases. As r1 decreases, the area of the cross section decreases to maintain the rate of flow.

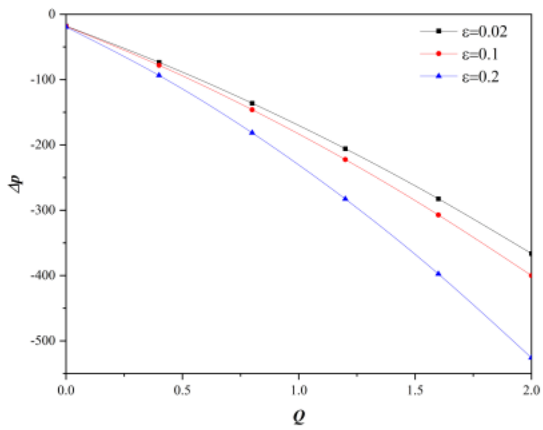

Figure 18: Pressure difference between wall vs. Flow rate

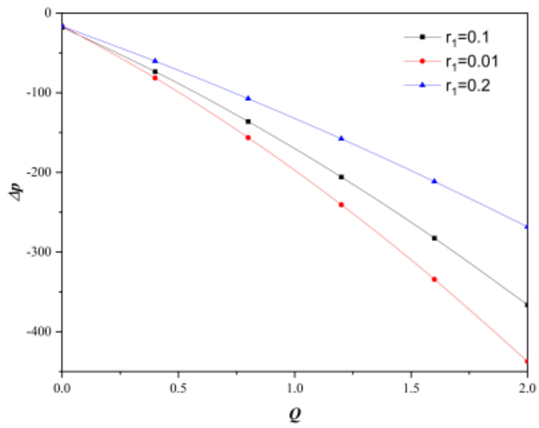

Figure 19: Pressure difference between wall vs. Flow rate

4. Conclusions

A theoretical analysis of heat transfer effects on peristaltic transport of viscoelastic Jeffrey fluid flowing in annulus created by concentric cylinders filled with fluid saturated porous media is presented. The coupled non-linear equations are subjected to regular perturbation. The simplified zeroth and first order equations are solved analytically. As Jeffrey parameter $\lambda \to 0$, the solution equals Newtonian fluid. Absence of heat transfer is marked by $G_m \to 0$. From the results, it is evident that permeability is not affecting significantly. Eckert number, inner tube radius, Jeffrey parameter are most influencing factors.

Acknowledgments

The authors extend their special thanks to the management of NMIT, Bengaluru - 560064 and ATMECE, Mysuru - 570028 for their unwavering cooperation in making this work possible.

Appendix

$$a_1 = \frac{\eta^2 - r_1^2}{\log\left(\frac{\eta}{r_1}\right)},$$

$$a_2 = \left[\frac{1+\lambda_1}{4}\right] P_{00}(x),$$

$$a_3 = \frac{\eta^2 - r_1^2}{4} + a_1^2 \log\left(\frac{r_1}{\eta}\right)\log(r_1\eta) + a_1\left(\eta^2 - r_1^2\right),$$

$$f_{11}(r,x) = \frac{r^6}{24} - \frac{\eta^4 r^2}{8} + a_1^2\left(\frac{r^2}{2}\right)\left[(\log r)^2 - \log r + \frac{1}{2} - (\log\eta)^2\right],$$

$$f_{12}(r,x)=a_1\left(\frac{r^4}{16}-\frac{\eta^2 r^2}{4}\right)-\frac{a^2}{\log\left(\frac{r_1}{\eta}\right)}\left(\frac{r^2}{4}\right)\left[\log\left(\frac{r}{\eta}\right)-1\right],$$

$$f(r,x)=f_{11}(r,x)-f_{12}(r,x),$$

$$f_{21}(r,x)=\frac{r^4}{4}\log\left(\frac{r}{\eta}\right)-\frac{r^8}{8}-a_1\left(\frac{r^2}{4}\right)-\left[\log\left(\frac{r}{\eta}\right)-1\right]+\frac{r^2}{8}-\frac{r^2 r_1^2}{2},$$

$$f_{22}(r,x)=\frac{a_1 r^2}{4}+\frac{a_1 r_1^2 r^2}{2}\left(\frac{a_2}{8\log\left(\frac{r_1}{\eta}\right)}\right),$$

$$f_2(r,x)=f_{21}(r,x)-f_{22}(r,x),$$

$$f_3(r,x)=\frac{r^2 r_1^2}{4}-\frac{r^4}{16}-a_1\left(\frac{r^2}{4}\right)\left[\log\left(\frac{r}{\eta}\right)-\frac{3}{4}\right],$$

$$a_6=\frac{f(r_1,x)-f(\eta,x)}{\log\left(\frac{r_1}{\eta}\right)},$$

$$b_{11}=-\frac{17}{1152}\eta^8-\frac{r_1^8}{1152}+\frac{\eta^4 r_1^4}{64}+a_1^2\left[\frac{3\eta^4}{8}-\frac{3r^4}{8}+\frac{r_1^4}{8}\log\left(\frac{r_1}{\eta}\right)\right]-a_1\left[\frac{\eta^4 r_1^4}{16}-\frac{15\eta^6}{96}-\frac{r^6}{96}\right],$$

$$b_{12}=\frac{a_3}{\log\left(\frac{r_1}{\eta}\right)}\left[\frac{7r_1^4}{32}-\frac{7\eta^4}{32}-\frac{r_1^4}{16}\log\left(\frac{r_1}{\eta}\right)\right],$$

$$f_8(r,x)=\frac{a_2 a_4 a_5}{\log\left(\frac{r_1}{\eta}\right)}\left[\frac{r^4}{16}\log\left(\frac{r}{\eta}\right)-\frac{5r^4}{32}\right]-a_1 a_2 a_4\left[\frac{r^6}{864}-\frac{\eta^4 r^2}{32}\right],$$

$$b_1=b_{11}-b_{12},$$

$$a_4=\left(\frac{1+\lambda_1}{2}\right)^2 P_{01},$$

$$a_5=a_2^2(1+\lambda_1),$$

$$a_7=\frac{f_3(r_1,x)-f_3(\eta,x)}{\log\left(\frac{r_1}{\eta}\right)},$$

$$f_4(r,x)=a_1^2 a_2 a_5\left[\frac{5r^4}{32}-\frac{r^4}{8}\log r\right]-a_1 a_2 a_5\left[\frac{r^6}{72}-\frac{\eta^2 r^4}{16}\right],$$

$$f_5(r,x)=a_2 a_4\left[\frac{r^4}{4}-a_1 r^2-\frac{a_1^2}{2}(\log r)^2\right]+a_2 a_5\left[\frac{r^8}{768}-\frac{\eta^4 r^4}{64}\right],$$

$$f_6(r,x)=a_1^3a_2a_5\left[\frac{5r^2}{16}-\frac{r^2}{4}\log r+\frac{r^2}{8}\right]+a_1{}^2a_2a_5\left[\frac{r^4}{64}-\frac{\eta^2r^2}{8}\right],$$

$$f_5(r,x)=\frac{a_1a_2a_4a_5}{\log\left(\frac{r_1}{\eta}\right)}\left[\frac{r^4}{4}\log\left(\frac{r}{\eta}\right)-\frac{3r^2}{4}\right]+a_1a_2^2a_5\frac{r^2}{2}-\frac{a_1^2a_2a_6}{2}(\log r)^2,$$

$$f_1(r,x)=f_5(r,x)+f_4(r,x)-f_8(r,x)+f_6(r,x)+f_7(r,x),$$

$$b_2=\frac{\eta^4r_1^2}{16}-\frac{\eta^6}{96}-\frac{r_1^6}{96}-a_1\left[\frac{r_1^4}{16}-\frac{\eta^4}{16}\log\left(\frac{r_1}{\eta}\right)-\frac{\eta^4}{16}\right],$$

$$a_8=\left[\frac{1+\lambda_1}{4}\right]P_{10}(x),$$

$$f_8(r,x)=2a_2a_8\left[\frac{r^4}{4}-a_1r^2-a_1^2\frac{(\log r)^2}{2}\right],$$

$$f_9(r,x)=(1+\lambda_1)a_2^2\left\{\frac{r_1^2r^4}{32}-\frac{r^6}{144}-a_1\left[\frac{r^4}{32}\log\left(\frac{r}{\eta}\right)-\frac{5r^4}{128}\right]-\frac{a_6r^2}{2}\right\},$$

$$f_{10}(r,x)=a_1\left(\frac{r_1^2}{8}-\frac{r^4}{64}\right)-a_1^2\left[\frac{r^2}{8}\log\left(\frac{r}{\eta}\right)-\frac{r^4}{32}\right]+a_2a_6\frac{(\log r)^2}{2},$$

$$f_4(r,x)=f_8(r,x)+f_9(r,x)+f_{10}(r,x),$$

$$a_9=\frac{f_4(r_1,x)-f_4(\eta,x)}{\log\left(\frac{r_1}{\eta}\right)}.$$

References

[1] S. K. Batra, Sperm transport through vas deferens: review of hypotheses and suggestions for a quantitative model, Fertility and Sterility 25(2) (1974), 186 – 202, doi:10.1016/s0015- 0282(16)40220-7.

[2] S. K. Guha, H. Kaur, and A. M. Ahmed Mechanics of spermatic fluid transport in the vas deferens, Med. and Biol. Engineering 13 (1975), 518 – 522, doi:10.1007/BF02477128.

[3] B. B. Gupta and V. Seshadri, Peristaltic pumping in non-uniform tubes, Journal of Biomechanics 9(2) (1976), 105 – 109, doi:10.1016/0021-9290(76)90130-5.

[4] L. M. Srivastava, and L. P. Srivastava, Peristaltic transport of a non-Newtonian fluid: Applications to the vas deferens and small intestine, Ann Biomed Eng. 13 (1985), 137 – 153, doi:10.1007/BF02584235.16

[5] T. W. Latham, Fluid motions in a peristaltic pump - MS Thesis, Massachusetts Institute of Technology., Dept. of Mechanical Engineering (1966), 30 – 35, https://hdl.handle.net/1721.1/17282.

[6] A. H. Shapiro, M. Y. Jaffrin and S. L. Wienberg, Peristaltic pumping with long wavelengths at low Reynolds number, Journal of Fluid Mechanics 37(4) (1969), 799 – 825, doi:10.1017/S0022112069000899.

[7] F. Yin and Y. C. Fung, Peristaltic Waves in Circular Cylindrical Tubes, Journal of Applied Mechanics 36(3) (1969), 579 – 589, doi:10.1115/1.3564720.

[8] J. C. Misra and S. K. Pandey, Peristaltic transport in a tapered tube, Mathematical and Computer Modelling 22(8) (1995), 137 – 151, doi:10.1016/0895-7177(95)00162-U.

[9] M. Li and J. Brasseur, Non-steady transport in finite-length tubes, Journal of Fluid Mechanics 248(1) (1993), 129 – 151, doi:10.1017/S0022112093000710.

[10] O. Eytan and D. Elad, Analysis of intra-uterine motion induced by uterine contractions, Bulletin of Mathematical Biology 61 (1999), 221 – 238, doi:10.1006/bulm.1998.0069.

[11] M. Mishra and A. R. Rao, Peristaltic transport of a Newtonian fluid in an asymmetric channel, Zeitschrift f¨ur angewandte Mathematik und Physik ZAMP volume 54 (2003), 532 – 550, doi:10.1007/s00033-003-1070-7.

[12] J. C. Misra and S. K. Pandey, Peristaltic transport of blood in small vessels: study of a mathematical model, Computers and Mathematics with Applications 43 (2002), 1183 – 1193, doi:10.1016/S0898-1221(02)80022-0.

[13] J. B. Shukla and S. P. Gupta, Peristaltic transport of a power-law fluid with variable consistency, Journal of Biomechanical Engineering 104(3) (1982), 182 – 186, doi:10.1115/1.3138346.

[14] K. K. Raju and R. Devanathan, Peristaltic motion of a non-Newtonian fluid, Rheological Acta 11 (1972), 170 – 178, doi:10.1007/BF01993016.

[15] A. V. Mernone, J. N. Mazumdar and S. K. Lukas, A mathematical study of peristaltic transport of a casson fluid, Mathematical and Computer Modelling 35(7-8) (2002), 895 – 912, doi:10.1016/S0895-7177(02)00058-4.

[16] T. Hayat, N. Ali and S. Asghar, Hall effects on Peristaltic flow of a Maxwell fluid in a porous medium, Physics Letters A 363(5-6) (2007), 397 – 403, doi:10.1016/j.physleta.2006.10.104.

[17] N. T. Eldabe, A. S. Zagrout, H. M. Shawky and Awad, Effecrs of chemical reaction with Heat and Mass transfer on Peristaltic motion of Power-law fluid in an asymmetic channel with Wall's properites, Int. J. Res. Appl. 15 (2013), 280 – 292, https://www.researchgate.net/publication/297771547.17

[18] A. Shaaban and M. Abouzeid, Effects of Heat and Mass Transfer on MHD Peristaltic Flow of a Non-Newtonian Fluid through a Porous Medium between Two Coaxial Cylinders, Mathematical Problems in Engineering (2013), doi:10.1155/2013/819683.

[19] C. K. Selvi, C. Haseena, A. N. S. Srinivas and S. Sreenadh, The effect of heat transfer on peristaltic flow of Jeffrey fluid in an inclined porous stratum, IOP Conference Series: Materials Science and Engineering 263(6), 1 – 15, (2017), doi:10.1088/1757- 899X/263/6/062027.

[20] A. M. Abdulhadi and T. S. Ahmed, Effect of radial magnetic field on peristaltic transport of Jeffrey fluid in curved channel with heat /mass transfer,IOP Conf. Series: Journal of Physics: Conf. Series 1003 (2018), 1 – 28, doi:10.1088/1742-6596/1003/1/012053.

[21] R. Indira, P. A. Dinesh and K. R. Sreegowrav, Effect of heat transfer on peristaltic flow of couple stress fluid in oesophagus, International Journal of Pure and Applied Mathematics 120 (2018), 1321 – 1335, https://www.acadpubl.eu/hub/2018-120-6/9/901.pdf.

[22] K. R. Rashmi, R. Indira and S. Jagadeesha, Peristaltic Flow of Couple-Stress Fluid in Doubly Connected Region with Reference to Endoscope, Palestine Journal of Mathematics 10 (2021), 1 – 5, https://www.researchgate.net/publication/353820386.

[23] I. Ramarao, P. N. Basavaraju and J. Seethappa, Effect of Heat Transfer on Peristaltic Transport of Prandtl Fluid in an Inclined Porous Channel, Mathematics and Computing. ICMC 2022. Springer Proceedings in Mathematics and Statistics 415 (2023), doi:10.1007/978-981- 19-9307-7-45.

[24] K. Vajravelu, G. Radhakrishnamacharya and V. Radhakrishnamurty, Peristaltic flow and heat transfer in a vertical porous annulus, with long wave approximation, International Journal of Non-Linear Mechanics 42(5) (2007), 754 – 759, doi:10.1016/j.ijnonlinmec.2007.02.014.